Article

Influence of Vinylene Carbonate and Fluoroethylene Carbonate on Open Circuit and Floating SoC Calendar Aging of Lithium-Ion Batteries

Karsten Geuder [1,*], Sebastian Klick [2], Philipp Finster [1], Karl Martin Graff [2], Martin Winter [3,4], Sascha Nowak [3], Hans Jürgen Seifert [1] and Carlos Ziebert [1,*]

[1] Institute for Applied Materials-Applied Materials Physics, Karlsruhe Institute of Technology (KIT), Hermann-von-Helmholtz-Platz 1, 76344 Eggenstein, Germany; philipp.finster@kit.edu (P.F.); hans.seifert@kit.edu (H.J.S.)

[2] Chair for Electrochemical Energy Conversion and Storage Systems, Institute for Power Electronics and Electrical Drives (ISEA), RWTH Aachen University, Campus Boulevard, 52074 Aachen, Germany; martin.graff@isea.rwth-aachen.de (K.M.G.)

[3] MEET Battery Research Center, University of Münster, Corrensstr. 46, 48149 Münster, Germany

[4] Helmholtz-Institute Münster, IEK-12, Forschungszentrum Jülich GmbH, Corrensstraße 46, 48149 Münster, Germany

* Correspondence: karsten.geuder@kit.edu (K.G.); carlos.ziebert@kit.edu (C.Z.)

Abstract: The purpose of this study was to investigate the calendar aging of lithium-ion batteries by using both open circuit and floating current measurements. Existing degradation studies usually focus on commercial cells. The initial electrolyte composition and formation protocol for these cells is often unknown. This study investigates the role of electrolyte additives, specifically, vinylene carbonate (VC) and fluoroethylene carbonate (FEC), in the aging process of lithium-ion batteries. The results showed that self-discharge plays a significant role in determining the severity of aging for cells without additives. Interestingly, the aging was less severe for the cells without additives as they deviated more from their original storage state of charge. It was also observed that the addition of VC and FEC had an effect on the formation and stability of the solid electrolyte interphase (SEI) layer on the surface of the carbonaceous anode. By gaining a better understanding of the aging processes and the effects of different electrolyte additives, we can improve the safety and durability of lithium-ion batteries, which is critical for their widespread adoption in various applications.

Keywords: lithium-ion batteries; calendar aging; electrolyte additives; vinylene carbonate; fluoroethylene carbonate; self-discharge

1. Introduction

Lithium-ion batteries (LIBs) have become a ubiquitous power source in today's world, powering everything from mobile devices to electric vehicles. However, one of the key challenges of LIBs is their limited cycle and calendar life, which can significantly affect their performance and safety over time. Calendar aging, in particular, is a major concern for LIBs, as it can cause irreversible degradation of the battery's capacity and increase the risk of safety hazards [1–3].

Calendar aging studies have been performed by many authors to model the aging behavior or to elucidate the mechanisms responsible for the reduced lifetime of LIBs [4–10]. The majority of calendar aging studies have been performed on commercial cells with graphite anodes and various cathode materials such as Li(NiMnCo)O$_2$ (NMC), Li(NiCoAl)O$_2$ (NCA), LiMn$_2$O$_4$ (LMO), LiFePO$_4$ (LFP), and LiCoO$_2$ (LCO). In contrast to known active materials, electrolytes and their additives are usually not specified. Ethylene carbonate (EC) is used as a solvent in LIBs, which exhibits a high dielectric constant to dissolve the inorganic salt [11]. Due to the relatively high melting point of EC (36 °C), it is mixed

with linear aliphatic carbonates such as dimethyl- (DMC), diethyl- (DEC), and/or methyl ethyl-carbonate (EMC). This mixture is combined with lithium-ion conductive salts such as $LiPF_6$ to form the electrolyte [11–13]. Calendar aging refers to the idle time of the battery, so the thermodynamic stability of the components governs the aging process [14]. Previous studies have shown a strong influence of temperature and the state of charge on the aging behavior. Ecker et al. [5] state an accelerated aging of NMC111/graphite cells for both high temperature and state of charge (SoC). This can be explained by the increased reaction rates induced by higher temperatures and the instability of the electrolyte, due to electrode/electrolyte reactions at high cell potentials [4]. The work of Schmalstieg et al. [10] used the same cells as Ecker et al. [5] at elevated temperatures and with a focus on high SoC resolution of 12 different SoCs in the range of 0 to 100%. Their study confirmed an increased capacity loss and resistance increase with higher storage SoC. Keil et al. [8] performed calendar aging tests on cells with different cathodes and graphite anodes. Their work revealed a non-linear influence of the SoC on calendar aging, resulting in plateau regions with a largely constant capacity fade. Dubarry et al. [4] reviewed calendar aging of graphite anodes with respect to various cathode materials. They found accelerated degradation for temperatures above 50 °C and storage SoCs greater than 60%. In addition, cells with NMC cathodes appeared to suffer greater degradation than those with NCA cathodes. Hahn et al. [7] studied 50.8 Ah NMC111 automotive cells and analyzed the capacity loss and volume change of the full cell during calendar aging. Their approach also considered the capacity loss due to the initial SEI growth during formation.

Calendar aging studies can be performed by charging or discharging the cells to the desired voltage [6] or SoC [15] and storing them at a certain temperature without compensation of voltage changes. In contrast to these so-called open circuit voltage (OCV) storage tests, the voltage can be kept at a fixed voltage level (floating SoC) [5]. Thus, voltage changes due to side reactions or self-discharge can be compensated [16]. Since most of the calendar aging studies used only one of the two methods, a direct comparison is difficult. Käbitz et al. [17] report significant differences only for 100% SoC.

One approach to mitigate calendar aging is to modify the battery's electrolyte by adding various additives. These electrolyte additives can improve the battery's performance by enhancing its electrochemical stability, preventing the formation of unwanted reaction products, and reducing the negative impact of side reactions [18–21]. However, the effect of these additives on the calendar aging of lithium-ion batteries is not well understood.

The electrochemical reduction of the electrolyte co-solvent ethylene carbonate (EC) during the initial formation cycles of the battery cell is crucial for the development of the passivating interphase [22]. Two widely used additives are vinylene carbonate (VC) and fluoroethylene carbonate (FEC), which are known to improve the performance of lithium-ion batteries. Several studies have reported that the addition of small amounts of VC or FEC to the electrolyte results in a reduction of SEI thickness, an improvement in cell capacity retention, and an increase in interphase temperature stability, while retaining the positive character of the SEI layer [21,23–26].

This paper aims to investigate the influence of the electrolyte additives VC and FEC on the calendar aging of lithium-ion batteries by OCV and floating SoC storage tests. The study focuses on evaluating the performance and aging behavior of batteries containing different electrolyte additives under various storage SoCs at 25 °C. The findings of this research could provide valuable insights into long-term reliability of lithium-ion batteries, regarding the influence of the two commonly used additives VC and FEC.

2. Materials and Methods

2.1. Cell Information

The high energy pouch cells used in this study were manufactured by an in-house battery production line and have a nominal capacity of 5.2 Ah and a nominal voltage of 3.7 V, with voltage limits of 3.0 V and 4.2 V. The anode material is graphite and the cathode material is $Li(Ni_{0.6}Mn_{0.2}Co_{0.2})O_2$ (NMC622). Utilized electrode materials were processed in

an in-house manufacturing plant. Active material for positive electrodes, i.e., NMC622, was coated onto aluminum foil (thickness: 15 μm) with conductive carbon and polyvinylidene difluoride in a ratio of 93/2/3 wt%, respectively. For negative electrodes, graphite (as active material), sodium carboxymethyl cellulose, and styrene butadiene rubber (ratio of 95.0/0.5/1.5 wt%, respectively) were coated onto copper foil (thickness of 10 μm). N-methyl-2-pyrrolidone was used as a processing solvent for positive electrodes, while the negative electrodes were processed with water. For NMC622, the chosen mass loading was 13.5 mg cm^{-2}, representing an aerial capacity of 2.3 mA h cm^{-2}. The chosen mass loading for graphite based electrodes was 7.9 mg cm^{-2}, resulting in an aerial capacity of 2.8 mA h cm^{-2}. Electrode sheets were calendared and dried under reduced pressure (120 °C; 1×10^{-3} mbar) for four days. To separate the electrodes, a Mitsubishi OZ-S30 separator (polyester non-woven separator with ceramic coating) was used. The base electrolyte is constituted of 1 M LiPF$_6$ in LP57 (EC:EMC = 3:7 wt%) and serves as a reference for the following aging tests. In order to investigate the influence of electrolyte additives on the calendar aging behavior, 5 wt% of either VC or FEC was added by the supplier (Solvionic, Toulouse, France) as two electrolyte variations. This amount was chosen to gain better understanding of the additives, although higher amounts of VC can have detrimental effects [27]. The cells were filled and sealed in a dry room with a dew point of -70 °C. An overview over the specific parameters of the cells in this study is given in Table 1. The aging study was performed with 8 cells per electrolyte composition. This results in a total number of 24 cells.

Table 1. Cell parameters for the pouch cells used in the aging studies.

Parameter	Value
Nominal capacity	5.2 Ah
Capacity used for charge and discharge protocol	5.0 Ah
Nominal voltage	3.7 V
End of charge, voltage	4.2 V
End of discharge, voltage	3.0 V

2.2. Formation

The calendar aging studies were carried out at different locations, with the use of different testing equipment. All electrochemical tests were performed with the exact same cycling parameters to ensure comparability. The formation cycle consisted of a charge step to the upper cut-off voltage of 4.2 V and a discharge step to the lower cut-off voltage of 3.0 V. Both the charge and discharge current were 1 A, which equals a C-rate of C/5. The temperature of the cells during formation was recorded with thermocouples type K. After the formation cycle, the cells were degassed and vacuum sealed in an argon-filled glove box (H$_2$O < 0.1 ppm, O$_2$ < 0.1 ppm). Within this process, gas samples were taken through a gas-tight syringe from the pouch bag of some cells and analyzed with a gas chromatography–mass spectrometry (GC-MS) system (Clarus 690 Arnel 5019, PerkinElmer LAS GmbH, Rodgau, Germany). The formation of the cells for the open-circuit storage tests was carried out using a BasyTec XCTS (BaSyTec GmbH, Asselfingen, Germany) test device. It was conducted inside a Binder KB 400 (Binder GmbH, Tuttlingen, Germany) temperature chamber at a temperature of 25 °C. The formation of the cells used in the floating SoC tests was carried out inside a Memmert (Memmert GmbH + Co. KG, Schwabach, Germany) temperature chamber with a Maccor 4200 battery cycler (Maccor Inc., Tulsa, OK, USA).

2.3. Test Setup

Prior to the calendar aging tests, the cells were cycled with a constant current of C/5 for 10 cycles to obtain a stable discharge capacity. This serves as begin of life (BoL) with the initial characterization test. The voltage–SoC characteristic for a C/10 discharge is shown in Figure 1. The three different electrolytes show very similar behavior and the corresponding voltages for the storage SoCs of 100%, 80%, 30%, and 5% are listed in Table 2.
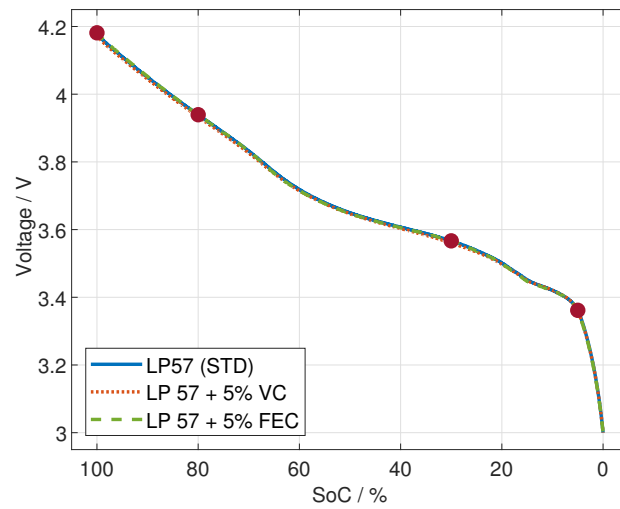
Figure 1. Comparison of C/10 discharge curves for all investigated cells with indicated storage SoCs, which were considered for the calendar aging study.

Table 2. SoC and corresponding voltages for varying electrolytes.

SoC	LP 57	LP 57 + 5% VC	LP 57 + 5% FEC
100%	4.18 V	4.18 V	4.19 V
80%	3.94 V	3.94 V	3.94 V
30%	3.57 V	3.56 V	3.56 V
5%	3.36 V	3.36 V	3.36 V

2.4. Characterization Tests

In order to quantify the aging and to gain insight into the degradation mechanisms, the cells were intermediately characterized every 4 months and compared to the values of the BoL test. This characterization is composed of a capacity check, a quasi-OCV cycle and pulse resistance measurements at two different SoCs (70% and 50%). The capacity test itself consists of a full charge with a rate of C/2, followed by a capacity check with a discharge rate of C/2. The values obtained from this capacity check are used as a measure of capacity fade in this publication. Additionally, cells are subjected to quasi-OCV charge and discharge cycles with a C-rate of C/10. Pulse tests at 1C current are performed at SoCs of 70% and 50% to determine the change in resistance during aging. Here the pulse resistance R_{pulse} is defined as follows:

$$R_{pulse} = \frac{|U(t_0) - U(t_0 + 10\text{s})|}{|I_{pulse}|} \tag{1}$$

The pulse tests were performed in both charge and discharge directions to negate any influence on the SoC. With a duration of 15 s, the change of SoC is less than 0.5%. The capacity measured during the capacity test was used to determine the storage SoC for the next storage period for OCV aging. Constant-voltage aging was always performed at the same voltages. After the cells were characterized, they were taken back to their storage chambers. The tests were designed to minimize the influence of the test while ensuring a sufficiently high resolution of the data.

2.4.1. (a) Open-Circuit Tests

The characterization tests for aging under OCV conditions were performed at 25 °C inside an Binder KB 400 (Binder GmbH, Tuttlingen, Germany) with a BioLogic BCS 815 battery cycler (Biologic, Seyssinet-Pariset, France). Prior to testing, the cells were allowed to thermally equilibrate for 2 h after removal from their storage locations to the

temperature (25 °C) of the characterization test. After the BoL characterization tests, the cells were charged to their respective storage SoC and stored in a Nüve ES120 (Nüve, Ankara, Turkey) temperature chamber at 25 °C for 4 months before they were characterized again. The calendar aging studies under OCV conditions were conducted for a total of 16 months.

2.4.2. (b) Floating SoC Tests

The floating SoC measurements were conducted using a Neware (Neware Technology Limited, Shenzhen, China) device in a Memmert temperature chamber (Memmert GmbH + Co. KG, Schwabach, Germany).

2.5. Self-Discharge

During open circuit calendar aging, a lithium-ion battery degrades over time, even when not in use. This results in less usable capacity and an increase in internal resistance. It is important to differ between irreversible and reversible capacity losses. An irreversible loss of capacity results from the loss of cyclizable lithium bound in the SEI [28]. Reversible capacity loss refers to the loss of charge over time due to various factors such as chemical reactions and leakage currents, a phenomenon commonly referred to as self-discharge. Self-discharge can cause the battery's SoC to decrease, resulting in degraded battery performance and reduced capacity. In the present calendar aging study under open-circuit conditions, the cells were not connected to any charging device and therefore the voltage decreased during storage. In contrast to these measurements, the floating SoC measurements were performed under constant-voltage conditions, where the cells are kept at a fixed voltage.

Similar to the assessment of self-discharge given by the work of Werner et al. [29], two different approaches were used. The first method uses the charge throughput, which is necessary to charge the cells to 100% after each storage period. The self-discharge (SD_x) of the aging period x is defined in Equation (2), as used by Werner et al. [29].

$$SD_x = \frac{C_{N,x-1} - (Q_{SoC,x-1} + Q_{100\%-SoC,x})}{C_{N,x-1}} < 0 \qquad (2)$$

The charge throughput $Q_{SoC,x-1}$ equals the amount of charge, which was used to charge to the desired storage SoC of the previous storage period. This is then added to charge throughput, which was needed to reach a full charge after the storage period. By dividing it by the cell capacity $C_{N,x-1}$, the self-discharge is normalized.

The second approach to measuring self-discharge is based on the change in voltage between subsequent storage periods. The voltage after the characterization test is compared with the voltage of the cells before the next check.

Self-discharge could not be analyzed for cells under constant voltage storage conditions.

3. Results and Discussion

3.1. Formation

For each electrolyte formulation, 8 cells were used, for a total of 24 cells. The formation procedure was carried out in the same way for all cells. The type of electrolyte used can affect the behavior of lithium ions and their interaction with the anode and cathode, resulting in different electrochemical reactions at different voltages [22]. A commonly used technique to improve battery performance is the addition of electrolyte additives. This method has been shown to increase battery life in both calendar and cycle terms, while reducing negative effects such as active lithium depletion during SEI formation and repair, electrolyte oxidation at the positive electrode, transition metal dissolution, and electrode damage [30,31].

Figure 2 shows an example of the first charge sequence during formation for the three different electrolyte combinations. The voltage curves are generally very similar. The magnifications in the potential window between 2 and 3.2 V show deviating voltage curves at the beginning of the very first charge sequence (SoC < 2%). Both FEC and VC

have a low Lowest Unoccupied Molecular Orbital (LUMO) level, which means that they are more easily reduced than EC at the interface between the anode and the electrolyte during the initial charging process [22]. These reduction processes appear as a change in the slope of the voltage vs. the SoC curve. They become even more apparent within a Incremental Capacity Analysis (ICA) of the formation process. The incremental capacity (*IC*) is calculated (Equation (3)) as the derivative of the capacity (*dQ*) with respect to the voltage (*dV*).
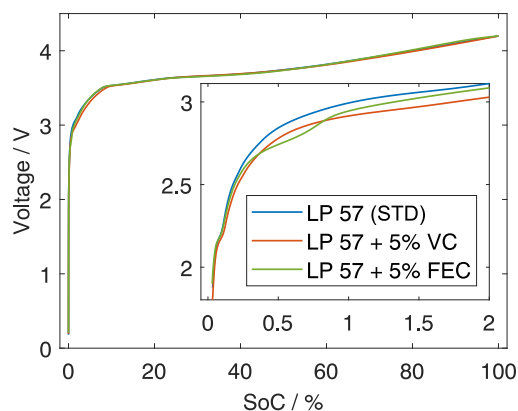
$$IC = \frac{dQ}{dV} \approx \frac{\Delta Q}{\Delta V} \tag{3}$$

Figure 2. Voltage vs. SoC curves for graphite/NMC622 cells with 1.0 M LiPF$_6$/EC:EMC 3:7 (STD), STD with 5 wt% VC, and STD with 5 wt% FEC.

Prior to the analysis, the raw voltage and capacity data were filtered to obtain fixed voltage intervals of 3 mV [32–34]. In Figure 3, the ICA for the first charge cycle is shown. The plot was created with the same data as for the charge vs. capacity plot. The first peak corresponds to the reduction of FEC at around 2.7 V. Secondly, VC is reduced at around 2.9 V, shortly before the EC from the standard electrolyte. This is in good agreement with the measurements from Nie et al. [24], who investigated very similar electrolyte combinations in graphite half cells. In addition, the work of Delp et al. [35] compared the same baseline electrolyte with different additives on the first charge cycle. They observed the same order of peaks, with FEC cells first, followed by FEC-filled cells before the final reduction peak of the baseline electrolyte.
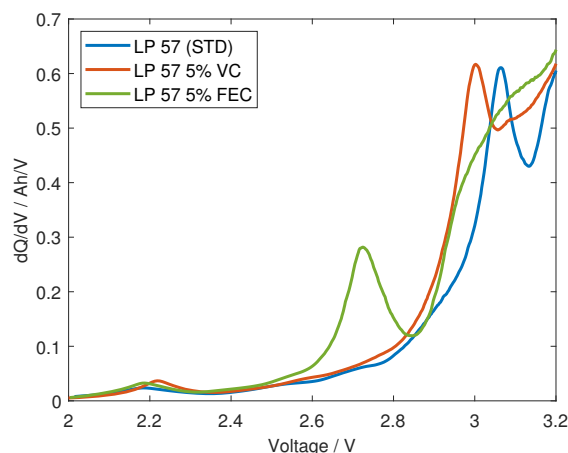

Figure 3. ICA of the formation charge step in the potential window between 2 V and 3.2 V.

Gas samples were taken from two cells of each type during the degassing and resealing of the pouch cells. They were qualitatively analyzed with gas chromatography–mass spectrometry (GC-MS). Table 3 lists the gaseous species, which were found in the different cells.

Table 3. Gas species detected after the formation cycle.

LP 57	LP 57 + 5% VC	LP 57 + 5% FEC
H_2, C_2H_4, C_2H_6, CH_4, CO, DMC, EMC, DEC	H_2, CO_2, C_2H_4, C_2H_6, CH_4, CO, EMC	H_2, CO_2, C_2H_4, C_2H_6, CH_4, CO

All samples contain H_2, C_2H_4, C_2H_6, CH_4, and CO. While the exact reaction mechanisms are still under discussion, various authors have reported CO_2 for both VC- and FEC-containing electrolytes [22–24,36,37]. This work confirms CO_2 as a product of VC- and FEC-containing electrolytes during formation.

3.2. Initial State

After the formation process, all 24 cells were cycled for 10 cycles at a current rate of C/5 at a temperature of 25 °C to obtain stable cell properties for a BoL characterization. This characterization consists of capacity tests and pulse current measurements. The values for the discharge capacity $C_{C/2}$ and the pulse resistance R_{pulse} listed in Table 4 are the initial values that will be used here to quantify aging.

Table 4. Initial state and deviation of the cells.

Parameter	LP 57	LP 57 + 5% VC	LP 57 + 5% FEC
$C_{C/2}$/Ah	5.02 ± 0.11	5.21 ± 0.08	5.17 ± 0.05
R_{pulse}/mΩ	15.26 ± 1.86	20.65 ± 0.53	12.34 ± 0.50

In terms of discharge capacity, the cells with additives show superior performance. The cells without additives exhibit an initial capacity of (5.02 ± 0.11) Ah, in contrast to (5.21 ± 0.08) Ah for the cells containing VC and (5.17 ± 0.04) Ah for FEC cells. Furthermore, the overall deviation of additive-free cells is considerably higher. Regarding the pulse resistance R_{pulse}, the cells with FEC feature the lowest values. Cells containing VC have the highest pulse resistance. High concentrations of VC were shown to exhibit a higher charge transfer resistance, especially at the graphite anode [19]. This can increase the resistance of the battery to the flow of lithium ions and reduce the battery's pulse power capabilities. On the other hand, FEC forms a thinner and more stable SEI layer, which allows for better lithium-ion transport and hence better pulse power performance. Burns et al. [19] conducted studies with varying VC content up to a maximum of 6%. Their work confirmed the beneficial effect of VC as an electrolyte additive, although they reported increased cell impedance for VC contents above 2% compared to the control electrolyte. The work of Hildenbrand et al. [27] used Bayesian optimization to improve the content of both VC and FEC as additives. They suggested a maximum of 5% of each additive for further study. Their studies also showed detrimental effects of VC concentrations above this threshold, while no such limitation was found for the use of FEC.

3.3. Self-Discharge

The mechanism of self-discharge in Li-ion batteries involves several chemical and electrochemical processes that can occur even when the battery is not in use [38]. One of the primary mechanisms of self-discharge is the reaction between the battery's electrodes and the electrolyte [39]. Over time, lithium ions can slowly migrate between the battery's electrodes, even when the battery is not in use. This can cause the battery's voltage to drop as a result of the gradual loss of charge. Another mechanism of self-discharge is the formation of side reactions within the battery. These side reactions can be caused by impurities in the battery materials or by other chemical processes that can occur within the battery [38].

The studied calendar aging was partially performed under OCV conditions. In this case, the cells were not recharged during the storage periods and self-discharge of the cells

was not prevented. Table 5 shows the maximum and average self-discharge rates during the storage period for all investigated storage conditions and electrolytes. The cells with pure LP57 suffered from severe self-discharge, which was most prominent at high SoCs. At an SoC of 100%, the maximum self-discharge was found to be 93%, which is attributed to a nearly complete discharge during a storage period of 4 months. For the cells stored at 30% and 5% SoC, the maximum self-discharge exceeded the actual state of charge, which can be explained by an increase in capacity during these storage periods, which will be further discussed in the following section.

Table 5. Self-discharge during storage for the investigated storage conditions and electrolyte combinations.

SoC	LP 57 Max./Avg.	LP 57 + 5% VC Max./Avg.	LP 57 + 5% FEC Max./Avg.
100%	93%/79%	2.9%/2.1%	4.8%/3.8%
80%	72%/65%	0.6%/0.2%	2.3%/1.5%
30%	42%/32%	0%/−0.3%	1.9%/0.9%
5%	9.9%/7.8%	1.1%/0.4%	0.7%/0.2%

The cells containing additives showed only moderate self-discharge. The cells with VC showed the lowest self-discharge. In general, the self-discharge was higher for higher SoCs.

Self-discharge in calendar aging experiments has been considered in previous studies [9,40]. These studies were performed using commercial Kokam cells with either NMC/graphite or NCA/graphite. The electrolyte and possible additives are not reported. It can be assumed that commercial batteries use sacrificial additives to improve their performance and therefore the results cannot be directly compared [22,41]. Zhang et al. [21] studied the self-discharge behavior of various electrolyte additives in NMC111/graphite cells with an unspecified electrolyte. They showed that over a storage time of 550 h, both small amounts of VC and FEC reduce the self-discharge, with VC being superior in terms of self-discharge compared to FEC.

Overall, the self-discharge process in lithium-ion batteries is complex and can involve several different mechanisms. The gradual loss of charge due to the migration of lithium ions between the battery's electrodes, the formation of side reactions, and the impact of temperature are factors that can contribute to a decrease in the cell voltage and an increase in the battery's self-discharge rate over time [42]. Recent research by Buechele et al. [43] attributed the self-discharge to the redox shuttle molecule dimethyl terephthalate (DMT). Their measurements showed that the addition of additives such as VC or FEC are able to suppress the undesired redox shuttle of DMT. Furthermore, Adamson et al. [44] showed that DMT is a decomposition product of the adhesive polyethylene terephthalate (PET) tape, which is used to secure the cell stack.

The self-discharge has a strong influence on the storage SoC. Its impact on the capacity and pulse resistance will be discussed in the next sections.

3.4. Capacity

3.4.1. OCV Conditions

Figure 4 shows the change in actual capacity over a 16-month period for all SoCs at 25 °C. The influence of the SoCs is obvious, resulting in faster degradation for cells stored at high potentials such as SoC100 or SoC80. This is in good agreement with the literature, where it has been shown that an increasing SoC causes a higher capacity loss [4,5,17,40].
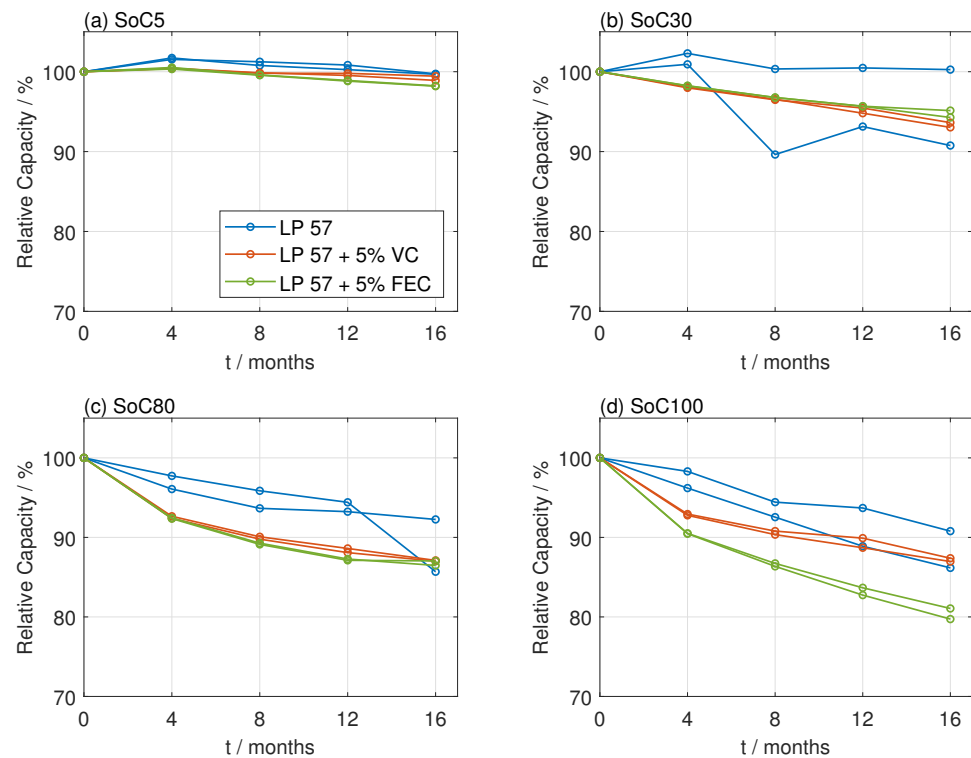
Figure 4. Evolution of discharge capacity from C/2 capacity test with regard to the electrolyte at the investigated SoCs of (**a**) SoC5, (**b**) SoC30, (**c**) SoC80, and (**d**) SoC100 at 25 °C under OCV conditions.

The cells at the lowest SoC (see Figure 4a) investigated show a very small capacity fade and during the first storage period a slight capacity increase can be observed for all electrolyte combinations. This can be attributed to the so-called "anode overhang effect", which can be responsible for a reversible capacity gain or loss [45]. The reversible capacity change is due to a geometrically larger anode compared to the cathode. The cells used in this study have an anode that overlaps the cathode by 1 mm on all sides. For a given lithium ion concentration gradient between the overhang and the part of the anode facing the cathode, lithium ions can migrate to or from the overhang, resulting in a measurable change in discharge capacity [46–49]. Prior to the start of the first storage period, the cells were at a SoC of 50% for a few days. Afterwards, the cells underwent BoL characterization and were charged or discharged to their storage SoCs. Therefore, the cells stored beneath this SoC exhibit a capacity increase, due to the overhang, and the cells stored at higher potentials suffer from a capacity loss. However, the aging processes overlap and are always dependent on the actual materials. The cells at SoC30 (see Figure 4b) show a higher capacity fade than those at SoC 5. One of the cells without additives shows a high capacity fade of about 10%, followed by an increase of almost 4%. After the second storage period, this explicit cell showed significant swelling of the pouch bag and was separated from the other cells and tested in a safe environment. The swelling disappeared after the characterization test and the cell was left in the test, in order to study the further gassing behavior. The other cell at SoC30 containing only LP57 showed superior performance and after one year of storage, the remaining capacity was nearly the same as at the beginning of the calendar aging tests. The cells with additives show quite similar capacity fade and the deviation between the cells is also very small. The cells stored at SoC80 (see Figure 4c) showed a higher degradation, with a capacity fade of more than 10% for the cells with additives and around 5% for those without additives. At the highest investigated SoC (see Figure 4d), which corresponds to a full charge, the cells with FEC show a significantly higher degradation. The VC cells show only small differences between SoC100 and SoC80. In general, the cells with additives show very similar degradation, while the pure LP57 cells show a larger scattering. The overall superior performance of the cells without VC and

FEC is quite counterintuitive, as previous studies have reported superior performance due to improved SEI formation from the addition of VC and FEC [50]. In this particular study, the cells exhibit such a high self-discharge that the actual storage SoC deviates greatly from the values set at the beginning of each storage period. This explains the smaller capacity fade in the cells without additives.

3.4.2. Floating SoC Conditions

Under constant voltage conditions, self-discharge does not influence the SoC value of the cell, as any decrease in cell voltage is compensated by an external current. Hence, no statement on the self-discharge of these cells can be made. Furthermore, the temperature of the oven was lower during the initial test, affecting initial capacity and resistance values. For storage at 3.35 V (see Figure 5a), an initial increase in capacity is observed, followed by a slow capacity fade for all cells, regardless of the electrolyte. However, the magnitude of this increase was higher in cells containing VC. In cells stored at 3.55 V (see Figure 5b), a similar behavior is visible: VC-containing cells exhibit an initial increase in capacity, followed by a decay. When stored at the upper cutoff voltage of 4.2 V (see Figure 5d), all cells suffer from substantial capacity fade. VC-containing cells exhibit the lowest fade, while FEC-containing cells, and one cell without additives loose over 10% of the initial capacity. Cells with VC stored at 3.9 V (see Figure 5c), corresponding to roughly 80% SoC, exhibit some initial capacity gain. For all storage conditions investigated, we can conclude that cells with VC lose less capacity.
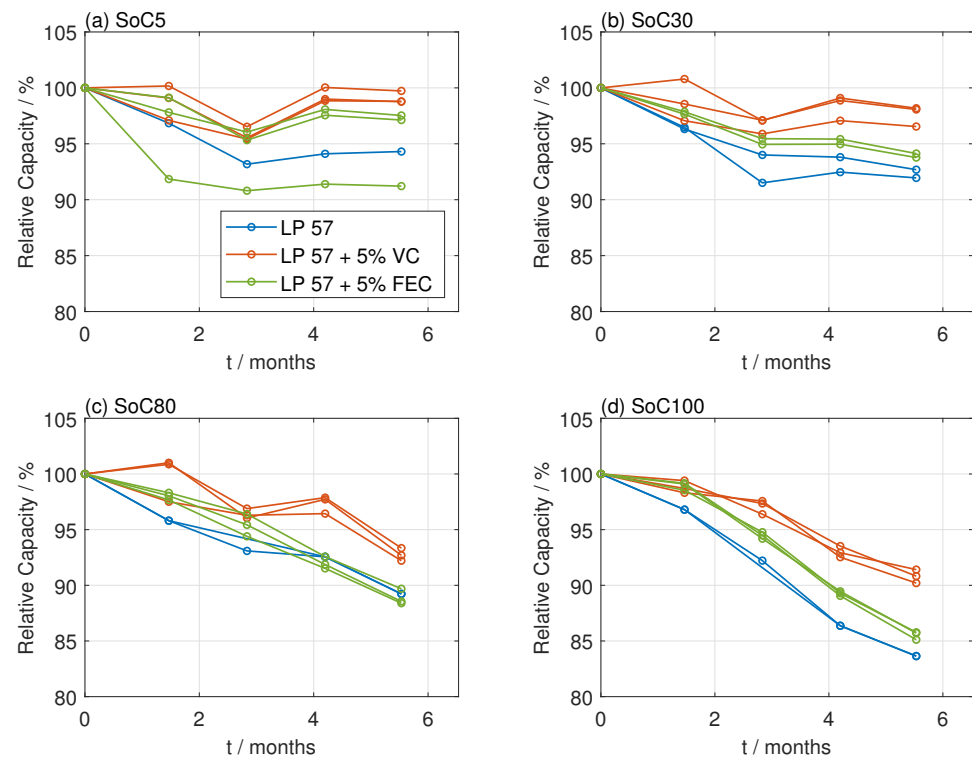

Figure 5. Evolution of discharge capacity from C/2 capacity test with regard to the electrolyte at the investigated SoCs of (**a**) SoC5, (**b**) SoC30, (**c**) SoC80, and (**d**) SoC100 at 25 °C under floating SoC conditions.

3.5. Resistance
3.5.1. OCV Conditions

In addition to the evaluation of capacity measurements, Figure 6 shows the increase in the pulse resistance in the pulse tests, which were carried out at 50% SoC. The pulse

resistance measurements for 70% SoC show similar trends. Thus, in the following, only the measurements for SoC50 will be taken into consideration.
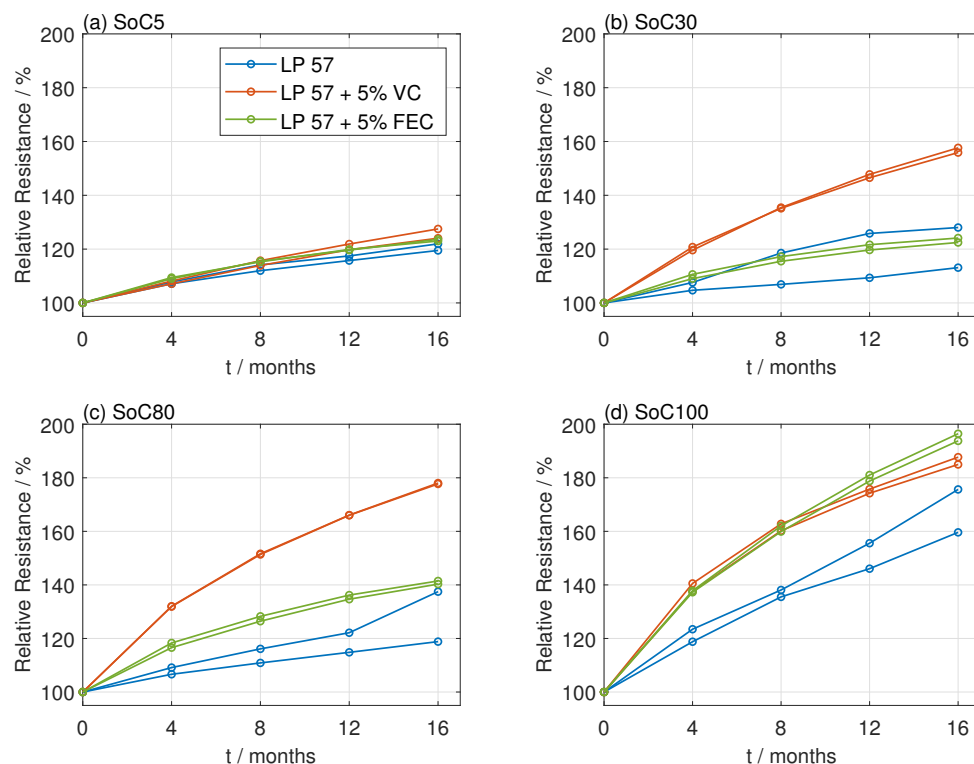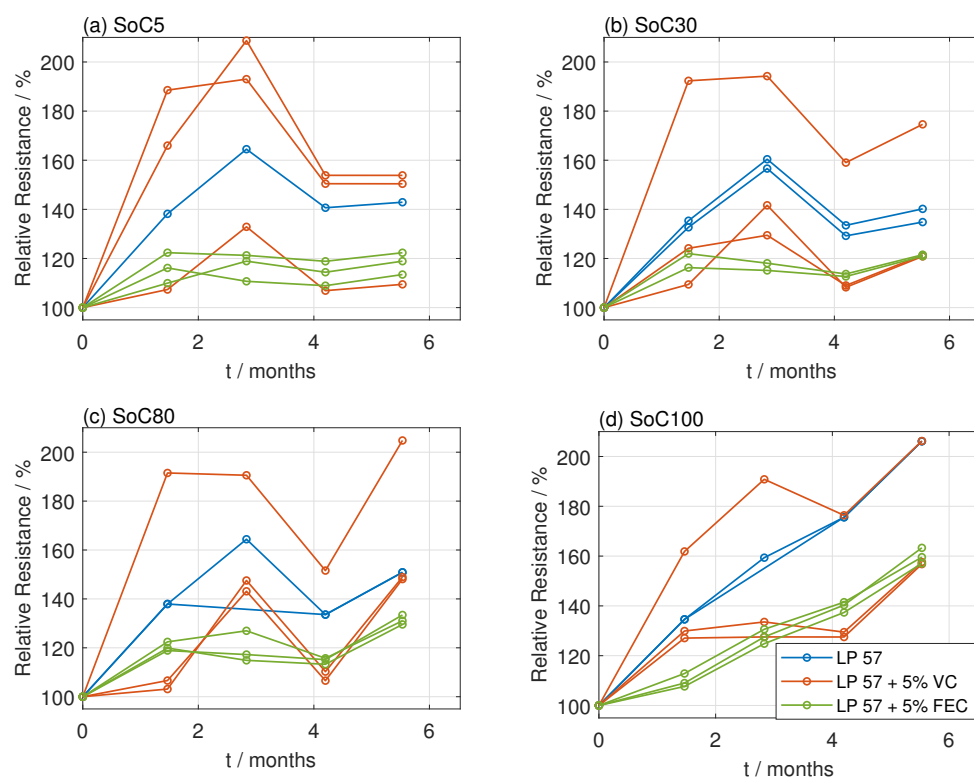

Figure 6. Pulse resistance rise evaluated from the pulse tests with regard to the electrolyte at the investigated SoCs of (**a**) SoC5, (**b**) SoC30, (**c**) SoC80, and (**d**) SoC100 at 25 °C under OCV conditions.

According to the qualitative analysis of the data, there are similar trends in the behavior of the battery over time with respect to its SoC. The data (see Figure 4) suggest that the aging process is more pronounced at higher potentials, such as SoC100 and SoC80. The pulse resistances show the same dependence as the capacity. The cells stored at SoC5 (see Figure 6a) show only minor differences among each other. The pulse resistance increased by 20% while the capacity remained constant. This can be explained by the simultaneous mechanisms of the migration of lithium ions from the anode overhang and degradation mechanisms. At SoC30 (see Figure 6b) and SoC80 (see Figure 6c), the cells with VC show the highest increase in pulse resistance. The cells with FEC increase by only 20% at SoC30. The cell that showed gassing during storage has a significantly higher increase in pulse resistance than the other cell under the same conditions. In general, VC is more stable than FEC at high potentials. The cells, which are charged to the upper cut-off voltage (see Figure 6d) show the highest resistance increase. This is due to the high potential, which is near the stability window of the electrolyte [17]. The cells without additives are self-discharging and are therefore only briefly exposed to the high potentials. When used with a carbonaceous anode, VC forms a stable SEI layer that is dense and uniform. This SEI layer is mainly composed of lithium alkyl carbonate species, which are formed through the reaction of VC with the lithium ions in the electrolyte. The lithium alkyl carbonate species have good mechanical strength and electrochemical stability, which help to protect the anode from further reactions with the electrolyte [22,51].

On the other hand, FEC forms a more porous and less stable SEI layer on the carbonaceous anode. This SEI layer is mainly composed of lithium fluoride and polymeric materials, which are formed through the reaction of FEC with the lithium ions in the electrolyte [22,51]. The polymeric materials in the SEI layer can be less stable and can contribute to the formation of a thicker SEI layer over time, which can reduce the performance and capacity of the battery.

3.5.2. Floating SoC Conditions

First, the measurements show a significant drop in relative resistance for some of the cells after the third characterization test, which can be explained by a change in temperature in the climate chamber from 20 °C to 25 °C. Due to the higher temperature, the internal resistance of the cells decreased.

Under constant voltage aging, cells without additives exhibit the highest relative resistance increase when considering the median of the tested cells at all conditions except 5%-SoC (see Figure 7). Under these conditions, the cells with 5% VC perform worse.

Figure 7. Pulse resistance rise evaluated from the pulse tests with regard to the electrolyte at the investigated SoCs of (**a**) SoC5, (**b**) SoC30, (**c**) SoC80, and (**d**) SoC100 at 25 °C under floating SoC conditions.

However, the spread of cells containing VC is very large. Two cells with VC show a high resistance increase at 5% SoC, while the third cell with VC at this SoC exhibits the lowest resistance increase of all cells. Cells with FEC exhibit lower resistance increase compared to cells without additives. Nie et al. [24] investigated the surface films with respect to electrolyte additives, and their work showed that the use of FEC results in a surface film that is rich in LiF and thinner than the SEI formed by their control electrolyte without additives.

A comparison with cells containing VC is challenging due to the large spread between these cells. Nevertheless, one explanation for the high impedance growth of VC cells may be the relatively high concentration of 5% VC [19,27]. A similar effect has not been reported for FEC. The difference in degradation between VC and FEC cells is due to the different composition and morphology of the SEI resulting from different reduction reactions and products [50]. The resistance increase of cells with FEC is approximately in the same range as the best-performing VC-containing cell.

Most of the studies on the effect of additives on the performance of LIBs have been conducted to investigate cycle life. Battery degradation cannot be assessed by cycle life alone because it always overlaps with calendar aging and both processes must be considered to improve battery performance and safety.

4. Conclusions

This study investigated the impact of electrolyte additives on the calendar aging of pouch cells with NMC622 cathodes and graphite anodes under different states of charge. Moreover, the two commonly used approaches of open-circuit and floating SoC calendar aging were compared for four different SoCs (SoC100, SoC80, SoC30, and SoC5). While there are several calendar aging studies on commercial lithium-ion batteries, most of them have focused on the electrode materials without detailed knowledge of the electrolyte and additives. Our studies aim to fill the gap in the literature between calendar aging on commercial cells and studies focused on the electrolyte system. In our case, both open-circuit and floating SoC calendar aging did not show similar degradation regarding the investigated electrolyte. The results showed that self-discharge played a critical role in determining the severity of aging in open circuit conditions for cells without additives. Interestingly, the aging was less severe for those cells without additives as they deviated from their original storage state of charge. Therefore the cells without additives were stored at significantly lower SoCs than the cells with VC and FEC. Under floating SoC conditions, the cell voltage is kept constant and the effects of self-discharge are mitigated. The floating SoC tests confirm better capacity retention for cells with electrolyte additives compared to the baseline electrolyte. In addition, cells with VC showed the least degradation for all SoCs tested.

For future research, a deeper understanding of the self-discharge mechanism is needed to better understand the impact of electrolyte additives on aging. It will also be interesting to investigate the effect of different temperatures on calendar aging, as this can significantly affect the stability of the battery. Overall, this study sheds light on the important role of electrolyte additives in battery aging, and highlights the need for further investigation to optimize the performance and durability of lithium-ion batteries.

Author Contributions: Conceptualization, K.G.; investigation, K.G., S.K., P.F. and K.M.G.; resources, S.N.; data curation, K.G. and S.K.; writing—original draft preparation, K.G. and S.K.; writing—review and editing, K.G., S.K., C.Z. and H.J.S.; visualization, K.G.; supervision, H.J.S., C.Z., M.W. and S.N.; project administration, H.J.S., C.Z., M.W. and S.N.; funding acquisition, H.J.S., C.Z., M.W. and S.N. All authors have read and agreed to the published version of the manuscript.

Data Availability Statement: Dataset available on request from the authors.

Conflicts of Interest: Author Martin Winter was employed by the Helmholtz-Institute Münster. The remaining authors declare that the research was conducted in the absence of any commercial or financial relationships that could be construed as a potential conflict of interest.

References

1. Garche, J.; Brandt, K. *Electrochemical Power Sources: Fundamentals, Systems, and Applications: Li-Battery Safety*; Electrochemical Power Sources; Elsevier: Amsterdam, The Netherlands; Kidlington, UK; Amebridge, PA, USA, 2019.
2. Essl, C.; Golubkov, A.W.; Gasser, E.; Nachtnebel, M.; Zankel, A.; Ewert, E.; Fuchs, A. Comprehensive Hazard Analysis of Failing Automotive Lithium-Ion Batteries in Overtemperature Experiments. *Batteries* **2020**, *6*, 30. [CrossRef]
3. Geisbauer, C.; Wöhrl, K.; Mittmann, C.; Schweiger, H.G. Review—Review of Safety Aspects of Calendar Aged Lithium Ion Batteries. *J. Electrochem. Soc.* **2020**, *167*, 090523. [CrossRef]
4. Dubarry, M.; Qin, N.; Brooker, P. Calendar aging of commercial Li-ion cells of different chemistries—A review. *Curr. Opin. Electrochem.* **2018**, *9*, 106–113. [CrossRef]

5. Ecker, M.; Nieto, N.; Käbitz, S.; Schmalstieg, J.; Blanke, H.; Warnecke, A.; Sauer, D.U. Calendar and cycle life study of Li(NiMnCo)O$_2$-based 18650 lithium-ion batteries. *J. Power Sources* **2014**, *248*, 839–851. [CrossRef]
6. Geisbauer, C.; Wöhrl, K.; Koch, D.; Wilhelm, G.; Schneider, G.; Schweiger, H.G. Comparative Study on the Calendar Aging Behavior of Six Different Lithium-Ion Cell Chemistries in Terms of Parameter Variation. *Energies* **2021**, *14*, 3358. [CrossRef]
7. Hahn, S.L.; Storch, M.; Swaminathan, R.; Obry, B.; Bandlow, J.; Birke, K.P. Quantitative validation of calendar aging models for lithium-ion batteries. *J. Power Sources* **2018**, *400*, 402–414. [CrossRef]
8. Keil, P.; Schuster, S.F.; Wilhelm, J.; Travi, J.; Hauser, A.; Karl, R.C.; Jossen, A. Calendar Aging of Lithium-Ion Batteries. *J. Electrochem. Soc.* **2016**, *163*, A1872–A1880. [CrossRef]
9. Redondo-Iglesias, E.; Venet, P.; Pelissier, S. Global Model for Self-Discharge and Capacity Fade in Lithium-Ion Batteries Based on the Generalized Eyring Relationship. *IEEE Trans. Veh. Technol.* **2018**, *67*, 104–113. [CrossRef]
10. Schmalstieg, J.; Käbitz, S.; Ecker, M.; Sauer, D.U. A holistic aging model for Li(NiMnCo)O$_2$ based 18650 lithium-ion batteries. *J. Power Sources* **2014**, *257*, 325–334. [CrossRef]
11. Kalhoff, J.; Eshetu, G.G.; Bresser, D.; Passerini, S. Safer Electrolytes for Lithium-Ion Batteries: State of the Art and Perspectives. *ChemSusChem* **2015**, *8*, 2154–2175. [CrossRef]
12. Nishi, Y. Lithium ion secondary batteries; past 10 years and the future. *J. Power Sources* **2001**, *100*, 101–106. [CrossRef]
13. Xu, K. Nonaqueous liquid electrolytes for lithium-based rechargeable batteries. *Chem. Rev.* **2004**, *104*, 4303–4417. [CrossRef] [PubMed]
14. Broussely, M.; Biensan, P.; Bonhomme, F.; Blanchard, P.; Herreyre, S.; Nechev, K.; Staniewicz, R.J. Main aging mechanisms in Li ion batteries. *J. Power Sources* **2005**, *146*, 90–96. [CrossRef]
15. Krupp, A.; Beckmann, R.; Diekmann, T.; Ferg, E.; Schuldt, F.; Agert, C. Calendar aging model for lithium-ion batteries considering the influence of cell characterization. *J. Energy Storage* **2022**, *45*, 103506. [CrossRef]
16. Lewerenz, M.; Käbitz, S.; Knips, M.; Münnix, J.; Schmalstieg, J.; Warnecke, A.; Sauer, D.U. New method evaluating currents keeping the voltage constant for fast and highly resolved measurement of Arrhenius relation and capacity fade. *J. Power Sources* **2017**, *353*, 144–151. [CrossRef]
17. Käbitz, S.; Gerschler, J.B.; Ecker, M.; Yurdagel, Y.; Emmermacher, B.; André, D.; Mitsch, T.; Sauer, D.U. Cycle and calendar life study of a graphite | LiNi$_{1/3}$Mn$_{1/3}$Co$_{1/3}$O$_2$ Li-ion high energy system. Part A: Full cell characterization. *J. Power Sources* **2013**, *239*, 572–583. [CrossRef]
18. Aurbach, D.; Gamolsky, K.; Markovsky, B.; Gofer, Y.; Schmidt, M.; Heider, U. On the use of vinylene carbonate (VC) as an additive to electrolyte solutions for Li-ion batteries. *Electrochim. Acta* **2002**, *47*, 1423–1439. [CrossRef]
19. Burns, J.C.; Kassam, A.; Sinha, N.N.; Downie, L.E.; Solnickova, L.; Way, B.M.; Dahn, J.R. Predicting and Extending the Lifetime of Li-Ion Batteries. *J. Electrochem. Soc.* **2013**, *160*, A1451–A1456. [CrossRef]
20. Wang, Y.; Nakamura, S.; Tasaki, K.; Balbuena, P.B. Theoretical studies to understand surface chemistry on carbon anodes for lithium-ion batteries: How does vinylene carbonate play its role as an electrolyte additive? *J. Am. Chem. Soc.* **2002**, *124*, 4408–4421. [CrossRef]
21. Zhang, S.S. A review on electrolyte additives for lithium-ion batteries. *J. Power Sources* **2006**, *162*, 1379–1394. [CrossRef]
22. Kitz, P.G.; Lacey, M.J.; Novák, P.; Berg, E.J. Operando investigation of the solid electrolyte interphase mechanical and transport properties formed from vinylene carbonate and fluoroethylene carbonate. *J. Power Sources* **2020**, *477*, 228567. [CrossRef]
23. Zhang, B.; Metzger, M.; Solchenbach, S.; Payne, M.; Meini, S.; Gasteiger, H.A.; Garsuch, A.; Lucht, B.L. Role of 1,3-Propane Sultone and Vinylene Carbonate in Solid Electrolyte Interface Formation and Gas Generation. *J. Phys. Chem. C* **2015**, *119*, 11337–11348. [CrossRef]
24. Nie, M.; Demeaux, J.; Young, B.T.; Heskett, D.R.; Chen, Y.; Bose, A.; Woicik, J.C.; Lucht, B.L. Effect of Vinylene Carbonate and Fluoroethylene Carbonate on SEI Formation on Graphitic Anodes in Li-Ion Batteries. *J. Electrochem. Soc.* **2015**, *162*, A7008–A7014. [CrossRef]
25. Intan, N.N.; Pfaendtner, J. Effect of Fluoroethylene Carbonate Additives on the Initial Formation of the Solid Electrolyte Interphase on an Oxygen-Functionalized Graphitic Anode in Lithium-Ion Batteries. *ACS Appl. Mater. Interfaces* **2021**, *13*, 8169–8180. [CrossRef]
26. McMillan, R.; Slegr, H.; Shu, Z.; Wang, W. Fluoroethylene carbonate electrolyte and its use in lithium ion batteries with graphite anodes. *J. Power Sources* **1999**, *81–82*, 20–26. [CrossRef]
27. Hildenbrand, F.; Aupperle, F.; Stahl, G.; Figgmeier, E.; Sauer, D.U. Selection of Electrolyte Additive Quantities for Lithium–Ion Batteries Using Bayesian Optimization. *Batter. Supercaps* **2022**, *5*, e202200038. [CrossRef]
28. Zhang, S.; Zhao, K.; Zhu, T.; Li, J. Electrochemomechanical degradation of high-capacity battery electrode materials. *Prog. Mater. Sci.* **2017**, *89*, 479–521. [CrossRef]
29. Werner, D.; Paarmann, S.; Wetzel, T. Calendar Aging of Li-Ion Cells—Experimental Investigation and Empirical Correlation. *Batteries* **2021**, *7*, 28. [CrossRef]
30. Smith, A.J.; Burns, J.C.; Xiong, D.; Dahn, J.R. Interpreting High Precision Coulometry Results on Li-ion Cells. *J. Electrochem. Soc.* **2011**, *158*, A1136–A1142. [CrossRef]
31. Downie, L.E.; Nelson, K.J.; Petibon, R.; Chevrier, V.L.; Dahn, J.R. The Impact of Electrolyte Additives Determined Using Isothermal Microcalorimetry. *ECS Electrochem. Lett.* **2013**, *2*, A106–A109. [CrossRef]

32. Krupp, A.; Ferg, E.; Schuldt, F.; Derendorf, K.; Agert, C. Incremental Capacity Analysis as a State of Health Estimation Method for Lithium-Ion Battery Modules with Series-Connected Cells. *Batteries* **2021**, *7*, 2. [CrossRef]

33. Zheng, L.; Zhu, J.; Lu, D.D.C.; Wang, G.; He, T. Incremental capacity analysis and differential voltage analysis based state of charge and capacity estimation for lithium-ion batteries. *Energy* **2018**, *150*, 759–769. [CrossRef]

34. Riviere, E.; Sari, A.; Venet, P.; Meniere, F.; Bultel, Y. Innovative Incremental Capacity Analysis Implementation for C/LiFePO$_4$ Cell State-of-Health Estimation in Electrical Vehicles. *Batteries* **2019**, *5*, 37. [CrossRef]

35. Delp, S.A.; Borodin, O.; Olguin, M.; Eisner, C.G.; Allen, J.L.; Jow, T.R. Importance of Reduction and Oxidation Stability of High Voltage Electrolytes and Additives. *Electrochim. Acta* **2016**, *209*, 498–510. [CrossRef]

36. Ota, H.; Sakata, Y.; Inoue, A.; Yamaguchi, S. Analysis of Vinylene Carbonate Derived SEI Layers on Graphite Anode. *J. Electrochem. Soc.* **2004**, *151*, A1659. [CrossRef]

37. Schwenke, K.U.; Solchenbach, S.; Demeaux, J.; Lucht, B.L.; Gasteiger, H.A. The Impact of CO$_2$ Evolved from VC and FEC during Formation of Graphite Anodes in Lithium-Ion Batteries. *J. Electrochem. Soc.* **2019**, *166*, A2035–A2047. [CrossRef]

38. Yazami, R.; Reynier, Y.F. Mechanism of self-discharge in graphite–lithium anode. *Electrochim. Acta* **2002**, *47*, 1217–1223. [CrossRef]

39. Utsunomiya, T.; Hatozaki, O.; Yoshimoto, N.; Egashira, M.; Morita, M. Self-discharge behavior and its temperature dependence of carbon electrodes in lithium-ion batteries. *J. Power Sources* **2011**, *196*, 8598–8603. [CrossRef]

40. Werner, D.; Paarmann, S.; Wiebelt, A.; Wetzel, T. Inhomogeneous Temperature Distribution Affecting the Cyclic Aging of Li-Ion Cells. Part II: Analysis and Correlation. *Batteries* **2020**, *6*, 12. [CrossRef]

41. Park, S.; Jeong, S.Y.; Lee, T.K.; Park, M.W.; Lim, H.Y.; Sung, J.; Cho, J.; Kwak, S.K.; Hong, S.Y.; Choi, N.S. Replacing conventional battery electrolyte additives with dioxolone derivatives for high-energy-density lithium-ion batteries. *Nat. Commun.* **2021**, *12*, 838. [CrossRef]

42. Wang, C.; Zhang, X.w.; Appleby, A.; Chen, X.; Little, F.E. Self-discharge of secondary lithium-ion graphite anodes. *J. Power Sources* **2002**, *112*, 98–104. [CrossRef]

43. Buechele, S.; Adamson, A.; Eldesoky, A.; Boetticher, T.; Hartmann, L.; Boulanger, T.; Azam, S.; Johnson, M.B.; Taskovic, T.; Logan, E.; et al. Identification of Redox Shuttle Generated in LFP/Graphite and NMC811/Graphite Cells. *J. Electrochem. Soc.* **2023**, *170*, 010511. [CrossRef]

44. Adamson, A.; Tuul, K.; Bötticher, T.; Azam, S.; Garayt, M.D.L.; Metzger, M. Improving lithium-ion cells by replacing polyethylene terephthalate jellyroll tape. *Nat. Mater.* **2023**, *22*, 1380–1386. [CrossRef]

45. Lewerenz, M.; Fuchs, G.; Becker, L.; Sauer, D.U. Irreversible calendar aging and quantification of the reversible capacity loss caused by anode overhang. *J. Energy Storage* **2018**, *18*, 149–159. [CrossRef]

46. Gyenes, B.; Stevens, D.A.; Chevrier, V.L.; Dahn, J.R. Understanding Anomalous Behavior in Coulombic Efficiency Measurements on Li-Ion Batteries. *J. Electrochem. Soc.* **2015**, *162*, A278–A283. [CrossRef]

47. Lewerenz, M.; Marongiu, A.; Warnecke, A.; Sauer, D.U. Differential voltage analysis as a tool for analyzing inhomogeneous aging: A case study for LiFePO$_4$ | Graphite cylindrical cells. *J. Power Sources* **2017**, *368*, 57–67. [CrossRef]

48. Lewerenz, M. *Sezierung und Quantitative Beschreibung der Alterung von Li-Ionen-Batterien Mittels Zerstörungsfreier Methoden Validiert Durch Post-Mortem-Analysen*; RWTH Aachen University: Aachen, Germany, 2018. [CrossRef]

49. Fath, J.P.; Alsheimer, L.; Storch, M.; Stadler, J.; Bandlow, J.; Hahn, S.; Riedel, R.; Wetzel, T. The influence of the anode overhang effect on the capacity of lithium-ion cells—A 0D-modeling approach. *J. Energy Storage* **2020**, *29*, 101344. [CrossRef]

50. Heiskanen, S.K.; Kim, J.; Lucht, B.L. Generation and Evolution of the Solid Electrolyte Interphase of Lithium-Ion Batteries. *Joule* **2019**, *3*, 2322–2333. [CrossRef]

51. Michan, A.L.; Parimalam, B.S.; Leskes, M.; Kerber, R.N.; Yoon, T.; Grey, C.P.; Lucht, B.L. Fluoroethylene Carbonate and Vinylene Carbonate Reduction: Understanding Lithium-Ion Battery Electrolyte Additives and Solid Electrolyte Interphase Formation. *Chem. Mater.* **2016**, *28*, 8149–8159. [CrossRef]